Recurrence of Intraseasonal Cold Air Outbreak during the 2009/2010 Winter in Japan and its Ties to the Atmospheric Condition over the Barents-Kara Sea

Masatake E. Hori[1], Jun Inoue[1], Takashi Kikuchi[1], Meiji Honda[1, 2], and Yoshihiro Tachibana[1, 3]
[1]*Research Institute for Global Change, JAMSTEC, Yokosuka, Japan*
[2]*Niigata University, Niigata, Japan*
[3]*Mie University, Tsu, Japan*

Abstract

In the winter of 2009/2010, Japan and the East Asian region experienced a frequent occurrence of cold air outbreaks. Although the winter average temperature in the Japan main islands was slightly positive (+0.81°C for DJF average and +0.71°C for NDJFM average), repeated decline in temperature was notable throughout the season. One explanation for this abnormal winter season is the extremely negative condition of the Arctic Oscillation (AO) that persisted from December to mid-January. However, AO alone does not provide sufficient explanation for the cold air outbreak during November or its intraseasonal periodicity. A case study of the cold air outbreak that reached Japan on Dec. 18 reveals an anomalous ridge forming over the Barents-Kara Sea, which leads to the cold air accumulation over western Siberia. The pressure anomaly subsequently shifted westward to mature into a blocking high which created a wave-train pattern downstream, advecting the cold air eastward towards East Asia and Japan. The sequence of events was also apparent in multiple cases throughout the season. This study suggests that there is a strong and systematic linkage in the intraseasonal timescale between the atmospheric condition over the Barents-Kara Sea and the cold air accumulation over the Eurasian continent, leading to the anomalous cold air outbreak over East Asia and Japan. The mechanism may also provide explanation to extreme winter conditions such as those observed during the winter of 2010/2011.

1. Introduction

The winter of 2009/2010 in Japan was marked by frequent surge of cold air. Figure 1a shows the surface temperature anomaly averaged over 58 JMA observatories excluding the southwest islands. The time series is smoothed using a 5-day running mean filter to remove the high frequency transients. While the temperature anomaly is moderately high with DJF average anomaly of +0.81°C and NDJFM average of +0.71°C, series of cold air outbreak persisted throughout the season. Due to this recurring cycle of cold air, the contrast of high/low temperature was strong, and a seasonal average of temperature is insufficient for representing the characteristic of this abnormal winter.

The index of AO (The definition is in section 2) in Fig. 1b shows that through much of December to February 2010, the index remained extremely negative. The DJF averaged AO index was −3.42, the lowest since 1977 which was −2.62. Negative AO is accompanied with high-pressure anomaly in the Arctic and low-pressure anomaly in the mid-latitudes, which amounts to cold Arctic air flowing into the mid-latitudes. In the seasonal scale, this negative AO is a good explanation for the observed negative temperature anomaly over the Eurasian continent, East Asia, and over North America. However, correlation between the temperature anomaly over Japan and the AO index is weak (r = 0.04), and neither does it explain the strong cold air outbreak that happened during November where the AO index was virtually neutral. While extremely negative AO certainly played a role in developing the cold air that frequented Japan, its periodicity in the intraseasonal timescale should be addressed under a different context.

There are two lines of studies that explain the contributing factor that leads up to the strong cold air outbreak in East Asia. One is the notion that ENSO related tropical variability plays a significant role in the development of the East Asian winter monsoon variability (Zhang et al. 1997; Lau and Nath 2000; Sakai and Kawamura 2009; Sakai et al. 2010). In this explanation, the winter monsoon is intensified through the changes in local Hadley circulation (Zhang et al. 1997) or through the upper tropospheric wave guide over South Asia (Sakai and Kawamura 2009), which induces the strong northwesterly seasonal wind in East Asia. The winter of 2009/2010 was a moderate El Niño, where the East Asian winter monsoon is known to become weaker due to the dampened convective activity over the tropical maritime continent, which is in contrast to the intense cold air outbreak that impacted Japan.

Another line of argument is the role of stationary Rossby waves in the Eurasian continent as an external forcing which in turn intensifies the surface Siberian high and the accompanying cold air outflow (Takaya and Nakamura 2005; Honda et al. 2009). One source of stationary Rossby waves is the existence of the Barents-Kara Sea. This ice-free ocean in the Arctic plays a significant role as a heat reservoir in which the summer induced heat is stored in the ocean and is subsequently released to the atmosphere during fall and winter (Screen and Simmonds 2010). Under the context of recent sea ice reduction (Inoue and Kikuchi 2007), such role of delayed atmospheric-ocean interaction between Autumn and Winter season is expected to become more prominent.

With these lines of argument in mind, the source of cold air during the 2009/2010 winter and the accompanying atmospheric

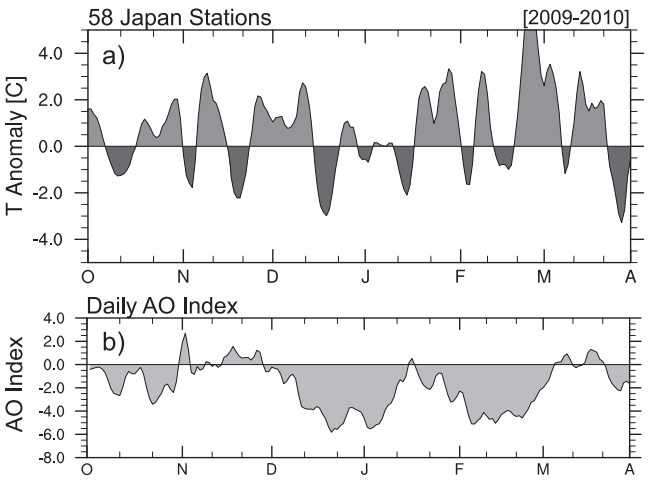

Fig. 1. Time series of (a) surface temperature anomaly averaged over 58 JMA observatory in the Japan main islands, and (b) the daily AO Index. 5-day running mean is used to suppress the transient fluctuations. Capital letters in the horizontal axis denote the start of a particular month.

Corresponding author: Masatake E. Hori, JAMSTEC/RIGC, 2-15 Natsushima-cyo, Yokosuka, Kanagawa 237-0061, Japan. E-mail: mehori@jamstec.go.jp.

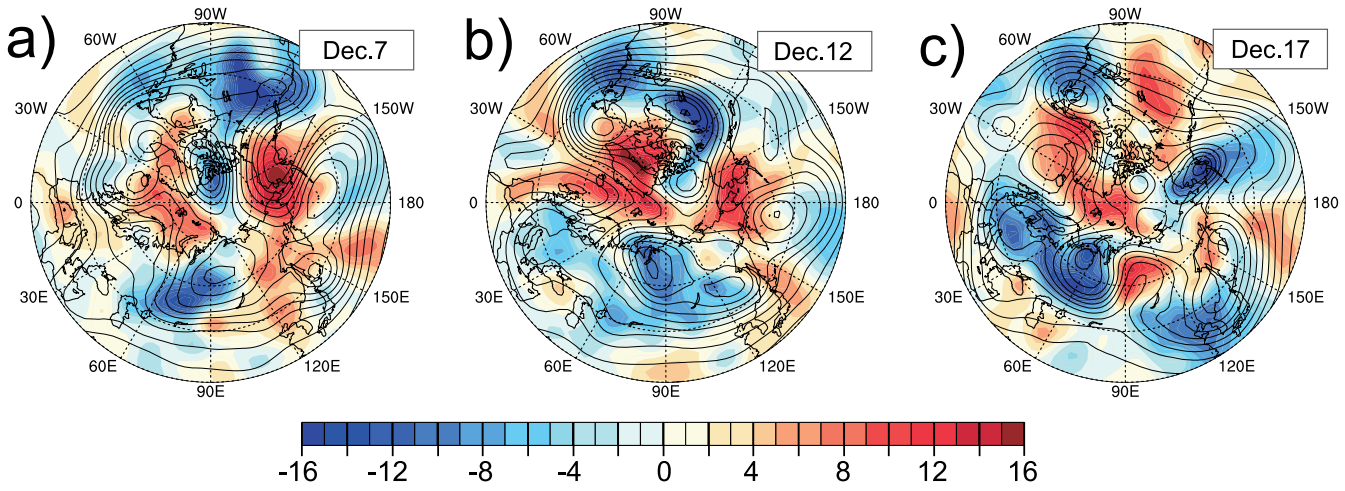

Fig. 2. 500 hPa geopotential height field (contour) and 850 hPa air temperature anomaly (shades) 10, 5, and 1 day prior to the arrival of the cold air in Japan for the case of December 18, 2009.

circulation is investigated through a case study and lag-regression analysis with the emphasis on the intraseasonal timescale.

2. Data

For an accurate assessment of the temperature fluctuation over Japan, daily values from all 58 Japan Meteorological Agency Observatory are used with an exception of 4 observatories residing in the southwest islands of Okinawa. The atmospheric data used in this study is the NCEP/NCAR (National Center of Environmental Prediction/National Center for Atmospheric Research) reanalysis dataset (Kalney et al. 1996). We use the geopotential height, air temperature and the surface sensible/latent heat fluxes where the spatial resolution is 2.5° × 2.5° regular latitude-longitude grid for the atmospheric data and T64 Gaussian grid for the surface fluxes. To examine the sub-monthly variability the daily data is used throughout this study. The AO index is provided by NOAA/CPC (National Oceanic and Atmospheric Administration/Climate Prediction Center) and is identified as the leading EOF mode of the 1000−700 hPa height anomaly north of 20°N. The definition is a slight variant from the original index proposed by Thompson and Wallace (2000) where a year-round monthly mean SLP is used instead of taking each month separately. The loading pattern is created based on years 1979−2000, and is projected on the following years to create a daily index. Apart from the AO index, the climatological mean is defined as an average of 1979−1999 throughout this study.

3. Results

From October 2009 to March 2010, there were 10 cases of cold air outbreaks reaching Japan (Fig. 1). Except for the case in mid-January, the negative peak is preceded by a positive temperature anomaly that drops rapidly within 6−10 days. Among these cases, Dec. 18 is marked to be the most intense, where the negative anomaly reached −3.47°C, the lowest in DJF average, and was preceded 6 days earlier by a warm anomaly of +4.94°C.

Figures 2a, b, and c shows the 500 hPa geopotential height and 850 hPa air temperature anomaly for 10 days, 5 days, and 1 day prior to the arrival of the cold air, respectively. 10 days prior to the arrival of the cold air, a ridge forms over the Barents Sea near 20°E−30°E, 70°N. Along with the strong blocking high located over Alaska, the height field in the Arctic region is predominantly high, contributing to the negative AO. The ridge over Barents Sea and the corresponding cyclonic anomaly give rise to the strong cold air advection from the Arctic towards western Siberia. The mass of cold air builds up along the trough region centered on 75°E, 50°N. In the following days, the ridge over Barents Sea shifts westward and matures as a blocking high over the North Atlantic Sea (Fig. 2b). On the other hand, the cold air mass moves eastward along with the movement of the trough. Finally, a strong wave train emanates downstream of the blocking, with a pressure anomaly along 60°E, 90°E, and 120°E respectively (Fig. 2c). The trough/ridge pattern is mostly in phase from the middle troposphere to the lower troposphere contributing the advection of cold air. In the days prior to the arrival of the cold air, the easternmost trough strengthens and advects the accumulated cold air that traveled from western Siberia across the Eurasian continent towards East Asia and Japan.

It is important to distinguish the role of the high pressure system over the Barents-Kara Sea and the succeeding blocking high, where the former is the driving mechanism behind the cold air accumulation, the latter and its associated wave pattern are responsible for advecting the accumulated cold air eastward. To further elucidate this point, the local heat advection and anomalous wind in the 850 hPa level for Dec. 7 are shown in Fig. 3. The local heat advection is calculated via a heat budget analysis following Tanaka and Milkovich (1990) using the formula:

$$\left[\frac{\partial c_p T}{\partial t}\right] = \left[-\mathbf{V}\cdot\nabla c_p T\right] + \left[\frac{c_p \gamma}{p}\omega\right] + [Q], \quad (1)$$

where the symbols denote the gravity constant g, area of the averaged region A, lower and upper pressure boundary p_s and

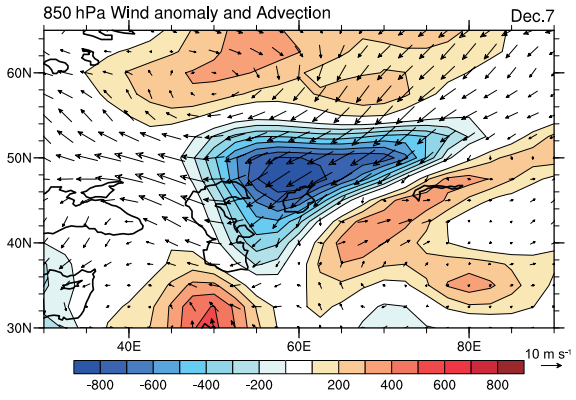

Fig. 3. Atmospheric heat advection vertically integrated up to 300 hPa (shades) and 850 hPa wind anomaly for December 7, 2009.

p_t which is set to 1000 hPa and 300 hPa respectively, horizontal wind vector **V**, pressure p, vertical p-velocity ω, static stability γ, specific heat at constant pressure c_p, temperature T, and diabatic heating rate Q. The bracket denotes the mass integration:

$$[*] = \frac{1}{gA}\int_A \int_{p_s}^{p_t} (*)\, dpdA. \qquad (2)$$

The advection term in Eq. (1) is used for the figures. It is evident that a strong cold air advection associated with the northeasterly wind is responsible for the accumulation of cold air in this region. The anticyclonic circulation anomaly is part of the ridge forming over the Barents-Kara sea, which drives the cold air from the Arctic and coastal Siberia.

Such chain of events is also visible for multiple cases of cold air outbreaks throughout the season. Figures 4a, b, and c shows the time series of 500 hPa geopotential height anomaly averaged over the Arctic including the Barents-Kara Sea (0°E−100°E, 70°N−90°N), the cold air accumulation over Western Siberia and its associated heat advection (40°E−100°E, 45°N−65°N), and the temperature anomaly over Japan (same as Fig. 1a), respectively. As in Fig. 1, all time series are smoothed using a 5-day running mean filter.

At least in 5 cases, the height anomaly over the Barents Sea coincides with the cold-air accumulation over Western Siberia, and a lag-relationship between the temperature over Japan is evident (shown in solid arrow). Two of these cases in November show a blocking over western Siberia and in the remaining cases, a blocking was visible over the North Atlantic. In the remaining cases, the relationship was only half visible, either the location of the cold air was displaced from western Siberia or the preceding height anomaly over the Barents Sea was not clear (shown in dashed arrows). The simultaneous correlation coefficient between the Barents-Kara Sea height anomaly and temperature anomaly over Western Siberia is −0.42, which is in the 99% confidence level based on a two-tailed Student-t test. Lag-correlation of air temperature anomaly over Japan lagging the Western Siberia by 9 days is 0.28, which is 90% significant. In cases where the lag-relationship is visible, a negative heat advection is visible prior to or in the beginning of the accumulation of cold air in western Siberia which suggests that the cold advection played a crucial role in the cold air accumulation.

To further elucidate the lag-relationship between the Arctic Sea and the cold air over the Eurasian continent, a lag-regression analysis is performed for the 500 hPa geopotential height and

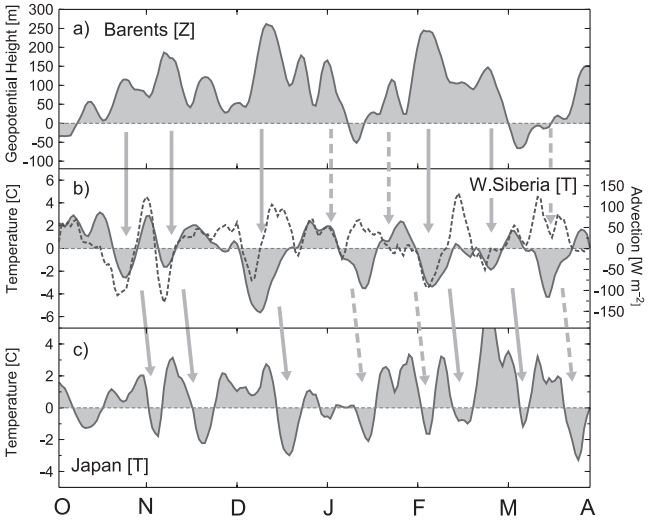

Fig. 4. Time series of (a) 500 hPa geopotential height anomaly averaged over the Arctic ocean covering the Barents-Kara Sea (0°E−100°E, 70°N−90°N), (b) 850 hPa temperature anomaly and heat advection (dashed line) averaged over western Siberia (40°E−100°E, 45°N−65°N), and (c) the surface temperature anomaly based on 58 JMA observatory in the Japan main islands. Capital letters in the horizontal axis denote the start of a particular month.

850 hPa air temperature against the surface temperature anomaly over Japan using the unfiltered 182 day time series starting from October 1 through March 30. Figures 5a, b, and c shows the atmospheric field leading 10 days, 5 days, and 1-day respectively with contours signifying the geopotential height and air temperature in shades. In Fig. 5a, the geopotential height over the Arctic is predominantly high with the center near the North Pole, just north of the Barents Sea. The anticyclonic anomaly associated with this high pressure advects cold air from the Arctic to the mid-latitudes where cold air is accumulated. It should be noted that each case of cold air accumulation takes place along the eastern fringe of the persisting ridge over the Barents-Kara Sea, which is not evident in the regression due to the fact that the regression was taken against the whole time series where features in each cases are canceled. A succession of trough/ridge pattern which matures into a wave

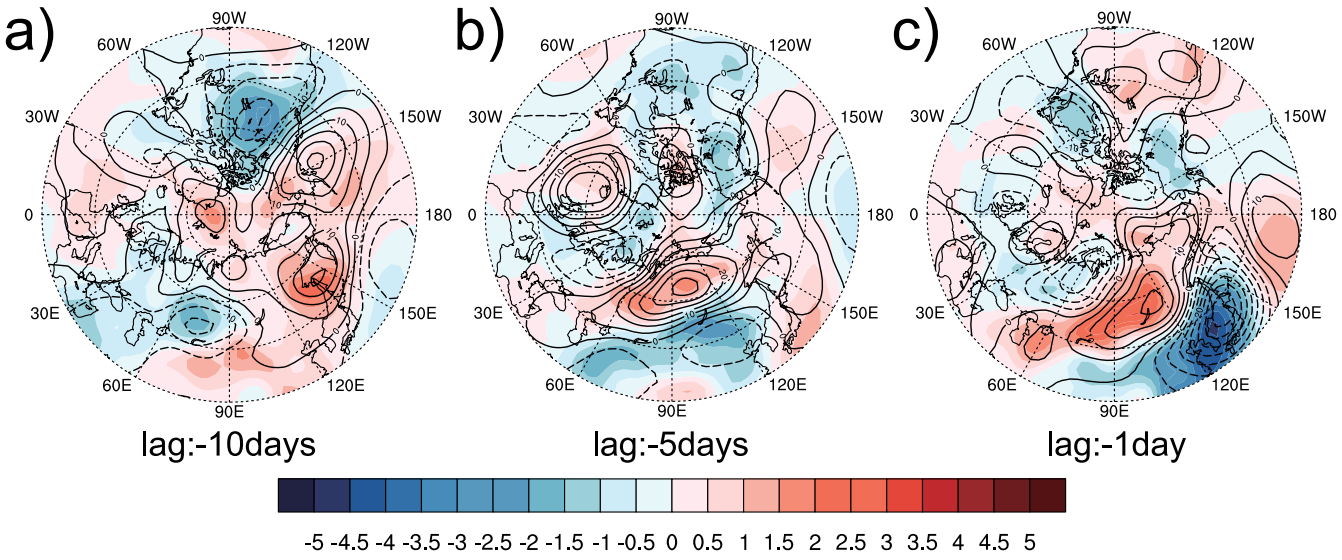

Fig. 5. Lag regression of 500 hPa geopotential height field (contour) and 850 hPa air temperature anomaly (shades) against the surface temperature anomaly over Japan corresponding to (a) 10 days, (b) 5 days, and (c) 1 day prior to the arrival of the cold air.

train is emerging along 10°W, 20°E, 50°E, 80°E. In the following days, the cold air anomaly elongates eastward along 45°N, which suggests that a topographical damming due to the Tibetan plateau plays a part in the development of this cold anomaly. The high pressure center near the North Pole shifts southwestward maturing into a blocking high. A succession of wave train emanating from the upstream of this blocking high across the Eurasian continent is evident in Figs. 5b, c. This is consistent with the findings of Takaya and Nakamura (2005) where the surface Siberian high is strengthened through the upper level wave train from the Atlantic Sea. The accumulated cold air moves eastward along with the intensifying East Asian trough and reaches Japan (Fig. 5c). On the heel of this cold air outbreak, a positive height anomaly accompanied by a large mass of warm air is positioned around 90°E−110°E, 50°N, which cancels the cold anomaly in the following days. Also, the next batch of cold air is already visible around 60°E, 60°N, thus creating the strong intraseasonal periodicity that is visible in Fig. 1a.

4. Discussion and summary

The strong intraseasonal temperature fluctuation that was observed in Japan during the 2009/2010 winter was brought forth by a distinctive chain of events. First, a persistent ridge is observed in the Arctic Sea, particularly over the Barents-Kara Sea. In multiple cases throughout this winter, this persistent ridge moved westward to mature into a strong blocking high over the North Atlantic and western Siberia. This persisting high pressure system is barotropic in nature and can be seen as a part of the overlying strong negative AO signature. The correlation between the Barents Sea high pressure (Fig. 4a) and the AO index (Fig. 1b) is −0.51 when the AO index lags the Barents-Kara Sea high anomaly by 3 days, which suggests that the intensification of the AO signature may partially be explained by the local changes in the Barents Sea region. Honda et al. (2009) supports this notion in which a reduced sea-ice distribution induces a localized heat flux anomaly, which in turn creates a high pressure anomaly over the Barents Sea. This localized anomaly generates a propagation of stationary Rossby waves and strengthens the Siberian High. Indeed, the sensible and latent heat flux anomaly during the winter season resembles Fig. 4 in Honda et al. (2009) which is a typical pattern of heat flux anomaly where the sea ice boundary retreats eastward far into the Kara sea (see Supplement 1). However, whether the ocean heat flux plays an active or passive role in inducing the atmospheric condition over the Barents-Kara Sea is unclear, and must be addressed in future research.

This study showed that while the storyline presented by Honda et al. (2009) holds true, the accumulating the cold air over the Eurasian continent and its successive advection in the intraseasonal timescale are a more accurate representation of the phenomenon.

Further study must be conducted to evaluate whether such scenario holds true for other years. Sakai and Kawamura (2009) pointed out that the combination of ENSO and North Atlantic Oscillation (NAO)-related forcing is crucial in the development of subpolar teleconnections over the Eurasian continent. The winter of 2009/2010 was a positive phase of ENSO, which statistically prefers a mild winter, but its relation to the frequency of strong cold air outbreak must be addressed. The relevance of this process in other severe winter years should be addressed, too. Takano et al. (2008) shows that a large-scale atmospheric dipole pattern resembling Fig. 5c consisting of a northern high covering Siberia and a southern low reaching East Asia was visible for the 2005 winter where the temperature was anomalously low in Japan. It should be noted that the severe winter condition during the 2010/2011 winter also resembled the pattern shown in Fig. 5.

The role of the diminishing sea ice must be addressed also. Screens and Simmonds (2010) points out that the heat input over the Arctic Ocean during the fall season is released to the atmosphere during the following season, contributing to much of the warming in the region. Strongest of such region is the Barents-Kara Sea where the trend in sea ice distribution during September is quite large. Due to the warming trend of the Arctic and the decreasing trend in sea ice distribution, such air-sea interaction will continue to be important in the coming years.

This mechanism introduces a possibility where warmer and reduced sea-ice in the Arctic may bring more extreme cold air outbreak in Japan and East Asia, which is contrary to normal expectations.

Acknowledgements

We would like to thank Dr. Yoshihiro Iijima for his valuable comments. We also thank two anonymous reviewers for their useful comments.

Supplement

Supplement 1 shows the sensible and latent heat flux anomaly averaged over the NDJFM winter season of 2009/2010.

References

Honda, M., J. Inoue, and S. Yamane, 2009: Influence of low Arctic sea-ice minima on anomalously cold Eurasian winters. *Geophys. Res. Lett.*, **36**, L08707, doi:10.1029/2008GL037079.

Inoue, J., and T. Kikuchi, 2007: Outflow of summertime Arctic sea ice observed by ice drifting buoys and its linkage with ice reduction and atmospheric circulation patterns. *J. Meteor. Soc. Japan*, **85**, 881−887.

Kalnay, E., and co-authors, 1996: The NCEP/NCAR 40-year reanalysis project. *Bull. Amer. Meteor. Soc.*, **77**, 437−471.

Lau, N. C., and M. J. Nath, 2000: Impact of ENSO on the variability of the Asian-Australian monsoons as simulated in GCM experiments. *J. Climate*, **13**, 4287−4309.

Sakai, K., R. Kawamura, and Y. Iseri, 2010: ENSO-induced tropical convection variability over the Indian and western Pacific oceans during the northern winter as revealed by a self organizing map. *J. Geophys. Res.*, **115**, D19125, doi: 10.1029/2010JD014415.

Sakai, K., and R. Kawamura, 2009: Remote response of the East Asian winter monsoon to tropical forcing related to El Niño -Southern Oscillation. *J. Geophys. Res.*, **114**, D06105, doi: 10.1029/2008JD010824.

Screen, J. A., and I. Simmonds, 2010: Increasing fall-winter energy loss from the Arctic Ocean and its role in Arctic temperature amplification. *Geophys. Res. Lett.*, **37**, L16707, doi:10.1029/2010GL044136.

Takano, Y., Y. Tachibana, and K. Iwamoto, 2008: Influences of large-scale atmospheric circulation and local sea surface temperature on convective activity over the Sea of Japan in December. *SOLA*, **4**, 113−116.

Takaya, K., and H. Nakamura, 2005: Mechanisms of intraseasonal amplification of the cold Siberian high. *J. Atmos. Sci.*, **62**, 4423−4440.

Tanaka, H. L., and M. F. Milkovich, 1990: A heat-budget analysis of the polar troposphere in and around Alaska during the abnormal winter of 1988/89. *Mon. Wea. Rev.*, **118**, 1628−1639.

Thompson, D. W. J., and J. M. Wallace, 2000: Annular modes in the extratropical circulation. Part I: Month-to-month variability. *J. Climate*, **13**, 1000−1016.

Zhang, Y., K. R. Sperber, and J. S. Boyle, 1997: Climatology and interannual variation of the East Asian winter monsoon: Results from the 1979−95 NCEP/NCAR reanalysis. *Mon. Wea. Rev.*, **125**, 2605−2619.

Manuscript received 22 October 2010, accepted 12 January 2011
SOLA: http://www.jstage.jst.go.jp/browse/sola/